

Communication

A PAIP Pincer Ligand Bearing a 2-Diphenylphosphinophenoxy Backbone

Kazuhiko Semba, Ikuya Fujii and Yoshiaki Nakao *

Department of Material Chemistry, Graduate School of Engineering, Kyoto University, Nishikyo-ku, Kyoto 615-8510, Japan; semba.kazuhiko.5n@kyoto-u.ac.jp (K.S.); fujii.ikuya.53m@st.kyoto-u.ac.jp (I.F.)

* Correspondence: nakao.yoshiaki.8n@kyoto-u.ac.jp; Tel.: +81-75-383-2443

Received: 15 August 2019; Accepted: 20 November 2019; Published: 28 November 2019



Abstract: A PAIP pincer ligand derived from 2-diphenylphosphino-6-isopropylphenol was synthesized. The Lewis acidity of the Al center of the ligand was evaluated with coordination of (O)PET₃. A zwitterionic rhodium-aluminum heterobimetallic complex bearing the PAIP ligand was synthesized through its complexation with [RhCl(nbd)]₂. Moreover, reduction of the zwitterionic rhodium-aluminum complex with KC₈ afforded heterobimetallic complexes bearing an X-type PAIP pincer ligand.

Keywords: pincer ligands; aluminum; heterobimetallic complexes

1. Introduction

Multidentate ligands containing an electropositive element have emerged recently to provide their transition-metal complexes with unique reactivity [1–4]. Among them, pincer ligands containing a group 13 element are of particular interest owing to their properties including: (1) electron-accepting ability as Z-type ligands through their vacant p orbitals and (2) high electron-donating ability as X-type ligands due to their low electronegativity [5–35]. Those bearing Al have gained much attention due to having the lowest electronegativity of Al among the group 13 elements [36], which could give X-type ligands with high Lewis acidity and electron-donicity (Figure 1). In this context, we previously reported on PAIP pincer ligand **1** and its rhodium complexes, which catalyzed C2-selective mono-alkylation of pyridine with unactivated alkenes through C(2)–H activation of pyridine coordinating to the Al center by the Rh center (Figure 1c) [20]. Herein, we report on PAIP pincer ligand **2** derived from 2-diphenylphosphino-6-isopropylphenol, expecting its Al center to be more Lewis acidic than that in **1** due to the higher electronegativity of oxygen compared to that of nitrogen (Figure 1d).

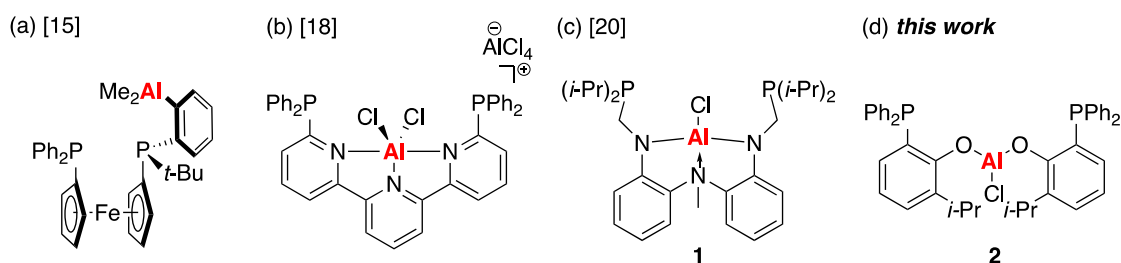
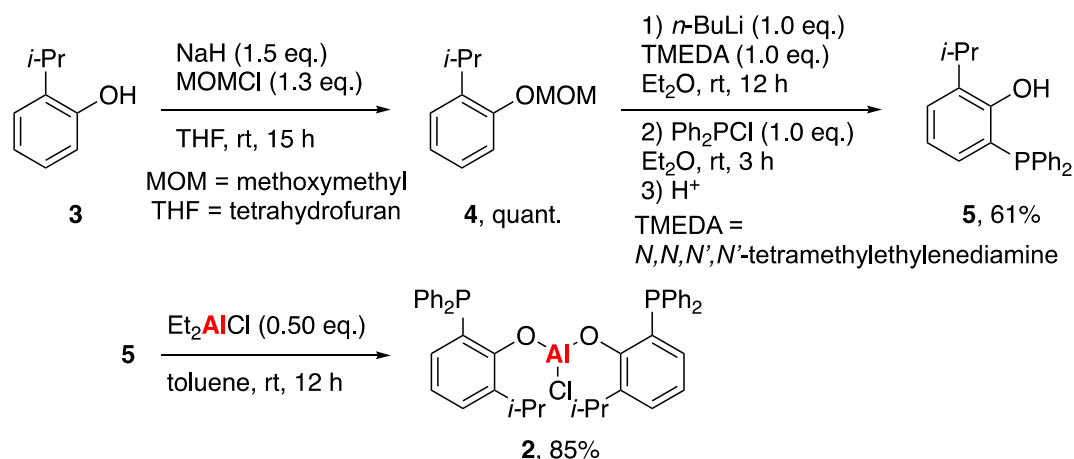


Figure 1. Reported pincer ligands containing an Al group in [15] (a), [18] (b), [20] (c) and this work (d).

2. Results and Discussion

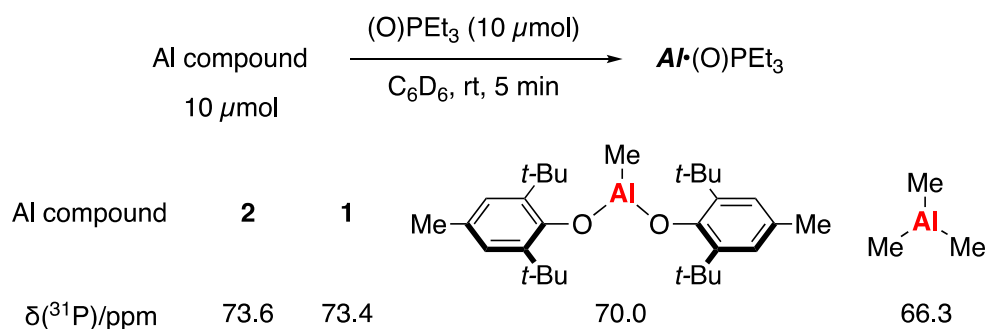
PAIP pincer ligand **2** was prepared from commercially available 2-isopropylphenol (**3**) in three steps (Scheme 1). Methoxymethylation of **3** with methoxymethyl chloride afforded

methoxymethyl (MOM)-protected 2-isopropylphenol **4**. Lithiation of **4** at the position *ortho* to the methoxymethoxy (OMOM) group with *n*-BuLi followed by the reaction with Ph₂PCl afforded 2-diphenylphosphino-6-isopropylphenol (**5**) in 61% yield. Finally, **2** was obtained by the reaction of Et₂AlCl with two molar equivalents of **5** in 85% yield.



Scheme 1. The preparation routine of PAIP pincer ligand **2**.

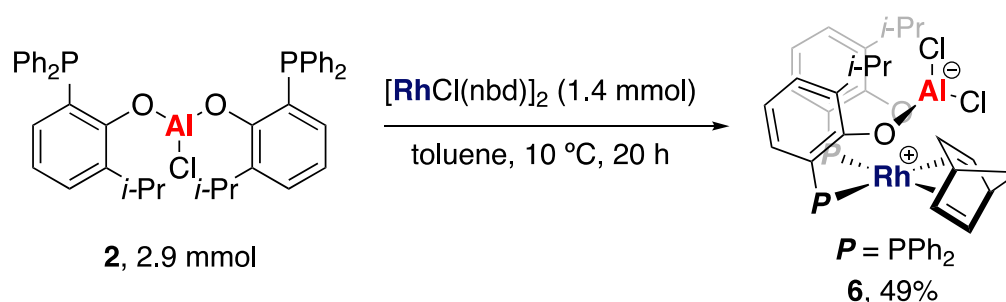
The Lewis acidity of **1** and **2** was evaluated and compared with common Al Lewis acids based on the method reported by Beckett (Scheme 2) [37,38]. The signal observed in ³¹P NMR spectrum of 2·(O)PEt₃ was in a magnetic field slightly lower than that of 1·(O)PEt₃, whereas those of the complexes from methylaluminum bis(2,6-di-*tert*-butyl-4-methylphenoxide) (MAD) [39,40] and AlMe₃ appeared in a much higher magnetic field. The diphenylphosphino groups in 2·(O)PEt₃ were observed equally, while the diisopropylphosphino groups in 1·(O)PEt₃ were observed unequally. This would suggest that one diisopropylphosphino group in 1·(O)PEt₃ coordinates to the Al center to afford penta- or hexacoordinated aluminum species. Although we cannot conclude whether **2** or **1** has a higher Lewis acidity due to the structural difference of the Al moiety between 2·(O)PEt₃ and 1·(O)PEt₃, the Lewis acidity of **2** is expected to be higher than MAD and AlMe₃.



Scheme 2. Evaluation of Lewis Acidity.

Coordination of **2** to transition metals to prepare heterobimetallic complexes was investigated next. As an example, the complexation of **2** with [RhCl(nbd)]₂ in toluene afforded a rhodium-aluminum complex **6** as an orange precipitate in high yield (Scheme 3). Single crystals were obtained by slow diffusion of *n*-hexane into a concentrated benzene solution of **6**. The crystal structure of **6** was revealed by X-ray diffraction analysis (Figure 2). In sharp contrast to the rhodium-aluminum complex bearing **1** as a supporting ligand, where the Al center acts as a neutral Z-type ligand [20], the Al moiety in **6** abstracts chlorine atom from the Rh center to generate a zwitterionic complex [5,12,28]. This could be

attributed to the structural flexibility and/or the higher Lewis acidity of the Al center in **2** compared to that in **1**.



Scheme 3. Preparation of a rhodium-aluminum complex **6**.

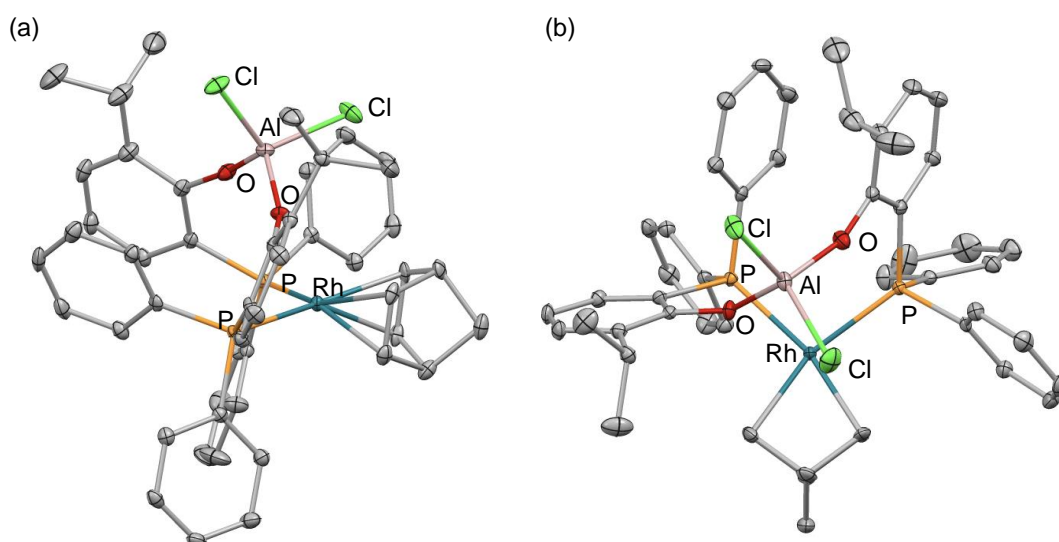
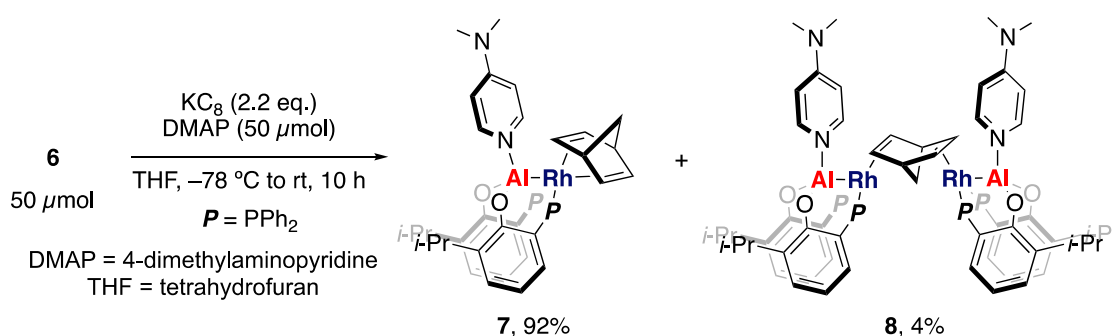


Figure 2. The crystal structure of **6**; (a) side view, (b) top view; thermal ellipsoids set at 30% probability; H atoms omitted for clarity.

A reduction of **6** with 2.2 equivalents of KC_8 in the presence of 4-dimethylaminopyridine (DMAP) afforded heterobimetallic complexes **7** and **8** in 92% and 4% yield, respectively (Scheme 4). Recrystallization by slow diffusion of *n*-pentane to a saturated benzene solution of a mixture of **7** and **8** generated crystals of **8**. An X-ray diffraction analysis of a crystal of **8** revealed that **2** became an X-type PAIP pincer ligand (Figure 3). Al in **8** would be formally served as an anionic Al(I) ligand, which is based on our knowledge that Al in an X-type PAIP pincer rhodium complex generated through a reduction of a rhodium complex bearing **1** by KC_8 was suggested to be an anionic Al(I) ligand by DFT calculations [20]. In the crystal structure, a distance between Rh and Al is 2.318 Å, which is shorter than the sum of the Van der Waals radii of Rh and Al [41]. Coordination of DMAP to the Al center indicates a Lewis acidity of the Al center. Double bonds of a norbornadiene were bridged over two rhodium centers to stabilize the electron-rich rhodium centers. A coordination site *trans* to the Al is vacant, which would result from strong σ -electron-donicity of the X-type Al ligand. Although all attempts to obtain crystals of **7** are failed, high resolution ESI mass spectrometry and the fact that addition of nbd (11 μmol) to a benzene solution of **8** (9.0 μmol) afforded **7** would support the structure of **7** as a heterobimetallic complex in which the Rh is chelated by a nbd ligand [20,42].



Scheme 4. Reduction of 6 to prepare 7 and 8.

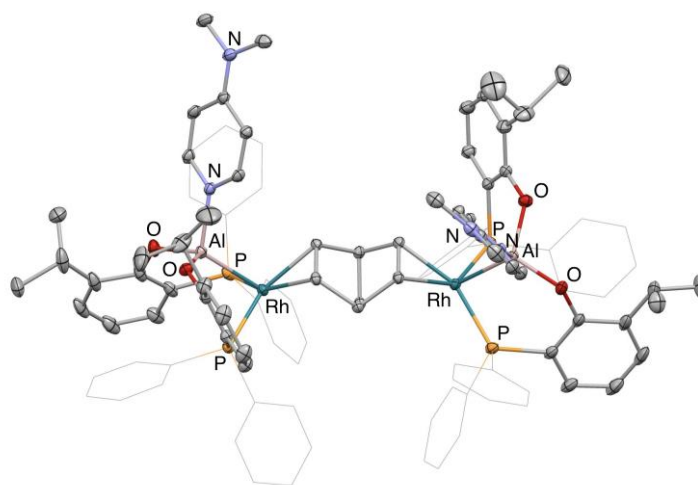


Figure 3. The crystal structure of 8; thermal ellipsoids set at 30% probability; carbon atoms on phosphorus atoms described in wireframes and H atoms omitted for clarity.

3. Materials and Methods

3.1. General

All manipulations of oxygen- and moisture-sensitive materials were conducted with a standard schlenk technique under an argon atmosphere or in a glove box under a nitrogen atmosphere. Medium pressure liquid chromatography (MPLC) was performed using Kanto Chemical silica gel 60 (spherical, 40–50 μm) (KANTO CHEMICAL CO., INC., Tokyo, Japan). Analytical thin layer chromatography (TLC) (Merck KGaA, Darmstadt, Germany) was performed on Merck TLC silica gel 60 F₂₅₄ (0.25 μm) plates. Visualization was accomplished with UV light (254 nm).

3.2. Apparatus

Proton, carbon, phosphorus, and aluminum nuclear magnetic resonance spectra (^1H , ^{13}C , ^{31}P , and ^{27}Al NMR) were recorded on a JEOL ECS-400 (^1H NMR 400 MHz; ^{13}C NMR 101 MHz; ^{31}P NMR 162 MHz; and ^{27}Al NMR 104 MHz) spectrometer (JEOL, Tokyo, Japan) with solvent resonance as the internal standard (^1H NMR, CDCl_3 at 7.26 ppm, CD_2Cl_2 at 5.32 ppm, C_6D_6 at 7.16 ppm; ^{13}C NMR, CDCl_3 at 77.0 ppm, CD_2Cl_2 at 53.8 ppm, and C_6D_6 at 128.0 ppm). NMR data are reported as follows: chemical shift, multiplicity (s = singlet, d = doublet, t = triplet, q = quartet, quint = quintet, sept = septet, br = broad, M = multiplet, and vt = virtual triplet), coupling constants (Hz), and integration. High resolution mass spectra were obtained with Thermo Scientific Exactive (ESI or APCI). Medium pressure liquid chromatography (MPLC) was performed with a Yamazen EPLC-W-Prep 2XY or SHOKO SCIENTIFIC Purif-espoir2. Elemental analyses were performed on a J-Science Micro corder JM10, JM11, and a YANACO Micro corder MT-6.

3.3. Chemicals

Unless otherwise noted, commercially available chemicals were used without further purification. $(\text{Rh}(\text{nbd})(\mu\text{-Cl}))_2$ (nbd = 2,5-norbornadiene) was synthesized following the reported procedure [43]. Anhydrous *n*-hexane, toluene, and THF were purchased from Kanto Chemical and purified by passage through activated alumina under positive argon pressure as described by Grubbs et al. [44]. Anhydrous *n*-pentane and benzene were purchased from FUJIFILM Wako Pure Chemical Corporation, and used after further dehydration with activated MS4Å.

3.4. Synthesis of 1-Isopropyl-2-Methoxymethoxybenzene (4)

To a suspension of sodium hydride (1.3 g, 55 mmol) in THF (20 mL), 2-isopropylphenol (3, 5.0 g, 37 mmol) in THF (20 mL) was added dropwise at 0 °C and the mixture was stirred for 10 min at the same temperature. To the resulting mixture, chloromethyl methyl ether (3.6 mL, 48 mmol) was added dropwise, and the mixture was stirred for 150 min at room temperature. After being quenched with H₂O, the mixture was extracted with Et₂O, and the combined organic layers were washed with 3 M NaOH aq. and dried over anhydrous MgSO₄. After filtration through a KIRIYAMA filter paper, the filtrate was concentrated in vacuo to give a colorless liquid (6.5 g). The product was used in the next step without further purification. ¹H NMR (400 MHz, CDCl₃): δ 1.27 (d, *J* = 6.9 Hz, 6H), 3.40 (sept, *J* = 6.9 Hz, 1H), 3.53 (s, 3H), 5.24 (s, 2H), 7.02 (dd, *J* = 7.3, 7.3 Hz, 1H), 7.10 (d, *J* = 7.8 Hz, 1H), 7.17 (dd, *J* = 7.8, 7.3 Hz, 1H), and 7.27 (d, *J* = 7.3 Hz, 1H). ¹³C{¹H} NMR (101 MHz, CDCl₃): δ 22.8, 26.8, 56.0, 94.4, 113.9, 121.8, 126.1, 126.6, 137.5, and 154.3. All the resonances of ¹H and ¹³C NMR spectra of the product were consistent with the reported values [45].

3.5. Synthesis of 2-Diphenylphosphino-6-Isopropylphenol (5)

To a solution of 4 (6.6 g, 37 mmol) in Et₂O (120 mL) we added tetramethylethylenediamine (5.5 mL, 37 mmol) and a solution of *n*-BuLi in *n*-hexane (1.6 M, 23 mL, 37 mmol) at −78 °C under an Ar atmosphere. The reaction mixture was allowed to warm up to room temperature and stirred for 12 h. To the mixture, chlorodiphenylphosphine (6.8 mL, 37 mmol) was added dropwise at 0 °C and the resulting mixture was stirred for 3 h at room temperature. All of the volatiles were removed under reduced pressure, and THF (40 mL) and 5 M HCl (40 mL) were added to the residue. The mixture was heated at 50 °C for 24 h, then neutralized using an aqueous NH₃ solution. The aqueous layer was extracted with Et₂O, and the combined organic layers were washed with water and dried over anhydrous MgSO₄. After filtration through a KIRIYAMA filter paper, the filtrate was concentrated under reduced pressure to give a pale yellow viscous liquid. The residue was purified by MPLC (ethyl acetate:*n*-hexane = 1:99) on silica gel to give a colorless viscous oil (7.2 g, 22 mmol, 61%). ¹H NMR (400 MHz, CDCl₃): δ 1.27 (d, *J* = 6.9 Hz, 6H), 3.33 (sept, *J* = 6.9 Hz, 1H), 6.54 (d, *J* = 8.7 Hz, 1H), 6.84–6.89 (m, 2H), 7.25 (t, *J* = 3.1 Hz, 1H), and 7.33–7.41 (m, 10H). ¹³C{¹H} NMR (101 MHz, CDCl₃): δ 22.5, 27.2, 120.1, 120.8 (d, *J* = 3.5 Hz), 128.3, 128.6 (d, *J* = 6.9 Hz), 128.9, 132.0 (d, *J* = 2.3 Hz), 133.4 (d, *J* = 18.5 Hz), 134.9, 135.1 (d, *J* = 4.6 Hz), and 156.7 (d, *J* = 19.7 Hz). ³¹P{¹H} NMR (162 MHz, CDCl₃): δ −30.2. HRMS-[APCI(+)] (*m/z*): [M + H]⁺ calcd for C₂₁H₂₂OP, 321.1403; found, 321.1407.

3.6. Synthesis of Bis(2-(Diphenylphosphino)-6-Isopropylphenoxy)-Aluminum Chloride (2)

To a solution of 5 (1.5 g, 4.7 mmol) in toluene (10 mL) we added a solution of diethylaluminum chloride in *n*-hexane (0.87 M, 2.7 mL, 2.3 mmol). The resulting solution was stirred for 12 h at room temperature, and all of the volatiles were removed in vacuo to afford the desired product as a white solid (1.4 g, 2.0 mmol, 85% yield). There would be two kinds of structural isomers (major:minor = 71:29). ¹H NMR (400 MHz, C₆D₆): δ major: 1.08 (d, *J* = 6.9 Hz, 12H), 3.13 (sept, *J* = 6.7 Hz, 2H), 6.76 (dd, *J* = 7.6, 7.6 Hz, 2H), 6.88–7.00 (m, 14H), 7.10 (t, *J* = 7.1 Hz, 2H), 7.24 (d, *J* = 7.3 Hz, 2H), 7.31 (br, 2H), 7.72 (br, 4H). minor: 1.12 (d, *J* = 6.9 Hz, 12H), 3.26–3.34 (m, 2H), 6.72 (dd, *J* = 7.6, 7.6 Hz, 2H), and 7.21 (d, *J* = 7.3 Hz, 2H). Other peaks were overlapped with those of the major isomer. ¹³C{¹H} NMR (101 MHz,

C_6D_6): δ 23.0, 23.4, 26.96, 26.98, 117.0, 117.4, 119.5, 120.1 (d, $J = 4.6$ Hz), 127.9, 128.4 (d, $J = 8.1$ Hz), 128.5, 128.8 (d, $J = 9.3$ Hz), 128.9, 129.0, 130.0, 130.8, 131.1, 131.3, 131.4, 134.0 (d, $J = 11.6$ Hz), 138.5, 138.7 (d, $J = 3.5$ Hz), 162.6 (d, $J = 23.1$ Hz), 163.4 (d, $J = 8.1$ Hz), and 163.6 (d, $J = 8.1$ Hz). $^{31}P\{^1H\}$ NMR (162 MHz, C_6D_6): δ -30.5 (minor), and -37.2 (major). $^{27}Al\{^1H\}$ NMR (104 MHz, C_6D_6): δ 65.6 (br) m.p. 119 °C.

3.7. Synthesis of 6

To a solution of $(Rh(nbd)(\mu-Cl)_2)$ (660 mg, 1.4 mmol) in toluene (5.0 mL), a solution of **2** (2.0 g, 2.9 mmol) in toluene (10 mL) was added at 10 °C. The reaction mixture was stirred for 20 h at 10 °C to give an orange precipitate. The orange precipitate was collected by filtration and washed with toluene (1.0 mL \times 3) and followed by *n*-pentane (2.0 mL \times 3). After being dried under reduced pressure, **6** was obtained as an orange solid (1.3 g, 1.4 mmol, 49%). Orange crystals for elemental analysis and X-ray diffraction analysis were obtained by a slow diffusion of *n*-hexane to a concentrated benzene solution of **6** at room temperature. 1H NMR (400 MHz, CD_2Cl_2): δ 1.15 (d, $J = 6.4$ Hz, 6H), 1.16 (d, $J = 6.9$ Hz, 6H), 1.38 (s, 2H), 3.59 (sept, $J = 6.6$ Hz, 2H), 3.76 (s, 2H), 4.00 (br s, 4H), 6.29–6.32 (m, 2H), 6.57 (t, $J = 7.6$ Hz, 2H), 7.01 (t, $J = 7.3$ Hz, 4H), 7.11 (d, $J = 7.3$ Hz, 2H), 7.19 (t, $J = 7.3$ Hz, 2H), 7.31–7.36 (m, 4H), 7.43–7.50 (m, 6H), and 7.59–7.63 (m, 4H). $^{13}C\{^1H\}$ NMR (101 MHz, CD_2Cl_2): δ 22.6, 24.4, 26.8, 51.7, 66.1, 74.8, 118.9 (vt, $J = 118.9$ Hz), 119.2 (vt, $J = 4.0$ Hz), 128.1 (vt, $J = 5.2$ Hz), 128.5 (vt, $J = 4.6$ Hz), 129.4, 129.7, 130.1, 130.5, 131.4 (vt, $J = 21.4$ Hz), 132.6 (vt, $J = 21.4$ Hz), 134.7 (vt, $J = 6.9$ Hz), 135.5 (vt, $J = 4.6$ Hz), 139.4, and 157.4 (vt, $J = 4.0$ Hz). $^{31}P\{^1H\}$ NMR (162 MHz, CD_2Cl_2): δ 23.3 ($J_{P-Rh} = 152.6$ Hz). $^{27}Al\{^1H\}$ NMR (104 MHz, CD_2Cl_2): δ 67.3 (br) Anal. Calcd $C_{49}H_{48}AlCl_2O_2P_2Rh$: C, 63.17; H, 5.19. Found: C, 63.00; H, 5.24. HRMS-[ESI(+)] (m/z): $[M+Na]^+$ calcd for $C_{49}H_{48}AlCl_2O_2P_2RhNa$, 953.1269; found, 953.1273. m.p. 157 °C (decomp).

3.8. Synthesis of 7 and 8

To a THF (4 mL) solution of **6** (50 mg, 50 μ mol) and 4-dimethylaminopyridine (7.0 mg, 50 μ mol), a suspension of potassium graphite (16 mg, 0.12 mmol) in THF (3 mL) was slowly added at -78 °C. The reaction mixture was stirred for 10 h at room temperature. THF was evaporated and benzene (10 mL) was added to the mixture. After filtration through a KIRIYAMA filter paper, the filtrate was concentrated to afford a brown precipitate. The precipitate was washed with *n*-pentane (3.0 mL \times 2) and dried under reduced pressure to give X-type rhodium-aluminum bimetallic complexes **7** and **8** as a brown solid in 92% and 4% yield (total 48 mg, 48 μ mol, 96%). Orange crystals of **8** for X-ray diffraction analysis were obtained by a slow diffusion of *n*-pentane to the concentrated benzene solution of a mixture of **7** and **8** at room temperature. All our attempts to obtain crystals of **7** failed.

7: 1H NMR (400 MHz, C_6D_6): δ 1.13 (d, $J = 7.3$ Hz, 6H), 1.29 (d, $J = 7.3$ Hz, 1H), 1.32 (d, $J = 6.4$ Hz, 6H), 1.44 (d, $J = 7.3$ Hz, 1H), 1.77 (s, 6H), 2.90 (s, 2H), 3.53 (br s, 2H), 3.58 (sept, $J = 6.7$ Hz, 2H), 4.62 (br s, 2H), 5.54 (d, $J = 7.3$ Hz, 2H), 6.81 (t, $J = 7.8$ Hz, 2H), 6.89–6.97 (m, 6H), 7.10 (t, $J = 7.3$ Hz, 2H), 7.15–7.21 (m, 6H), 7.24 (d, $J = 7.3$ Hz, 2H), 7.49–7.56 (m, 6H), and 8.07–8.12 (m, 4H). $^{13}C\{^1H\}$ NMR (101 MHz, C_6D_6): δ 22.8, 23.5, 27.3, 37.9, 40.8 (vt, $J = 8.1$ Hz), 40.9 (vt, $J = 7.5$ Hz), 49.2, 63.4, 98.1, 105.7, 118.0, 123.9 (vt, $J = 23.7$ Hz), 127.0, 127.2, 127.4, 127.9, 130.7, 133.1 (vt, $J = 6.4$ Hz), 134.4 (vt, $J = 7.5$ Hz), 138.4, 139.4 (vt, $J = 12.1$ Hz), 145.4 (vt, $J = 16.8$ Hz), 146.1, 154.8, and 161.3 (vt, $J = 5.8$ Hz), an sp^2 carbon signal overlaps with others. $^{31}P\{^1H\}$ NMR (162 MHz, C_6D_6): δ 27.0 ($J_{P-Rh} = 157.0$ Hz). $^{27}Al\{^1H\}$ NMR (104 MHz, C_6D_6): it is too broad to identify the corresponding signal. Elemental analysis did not give a satisfactory result due to instability of **7** toward O_2 and H_2O . HRMS-[ESI(+)] (m/z): $[M]^+$ calcd for $C_{56}H_{58}AlN_2O_2P_2Rh$, 982.2838; found, 982.2834. m.p. 165 °C (decomp).

8: 1H NMR (400 MHz, C_6D_6): δ -0.69 (s, 2H), 1.19 (d, $J = 6.4$ Hz, 12H), 1.29 (d, $J = 6.9$ Hz, 12H), 1.84 (s, 12H), 3.04 (s, 4H), 3.07 (s, 2H), 3.49 (sept, $J = 6.6$ Hz, 4H), 5.16 (d, $J = 6.0$ Hz, 4H), 6.76 (t, $J = 7.3$ Hz, 4H), 6.93–6.96 (m, 22H), 7.12–7.17 (m, 6H), 7.20 (d, $J = 7.3$ Hz, 4H), 7.47 (d, $J = 6.0$ Hz, 4H), 7.50–7.57 (m, 8H), and 7.83–7.91 (m, 8H). $^{13}C\{^1H\}$ NMR (101 MHz, C_6D_6): δ 22.9, 23.3, 27.7, 38.1, 47.0, 58.9, 67.1 (br), 105.7, 118.1, 124.7, 125.2, 126.8, 130.4, 133.4 (br), 134.4 (vt, $J = 6.9$ Hz), 137.8, 140.5 (vt, $J = 22.5$ Hz), 146.2, 154.8, and 160.8 (vt, $J = 6.4$ Hz). $^{31}P\{^1H\}$ NMR (162 MHz, C_6D_6): δ 24.1 ($J_{P-Rh} =$

139.5 Hz). $^{27}\text{Al}\{^1\text{H}\}$ NMR (104 MHz, C_6D_6): it is too broad to identify the corresponding signal. Anal. Calcd $\text{C}_{105}\text{H}_{108}\text{Al}_2\text{N}_4\text{O}_4\text{P}_4\text{Rh}_2$: C, 67.31; H, 5.81; N, 2.99. Found: C, 66.35; H, 5.82; N, 2.50. Elemental analysis did not give a satisfactory result due to instability of **8** toward O_2 and H_2O . HRMS–[ESI(+)] (m/z): $[\text{M}]^+$ calcd for $\text{C}_{105}\text{H}_{108}\text{Al}_2\text{N}_4\text{O}_4\text{P}_4\text{Rh}_2$, 1872.5056; found, 1872.5005. m.p. 169 °C (decomp).

3.9. Evaluation of Lewis Acidity of Aluminum Compounds

In a glove box, aluminum compound (10 μmol) and the triethylphosphine oxide (10 μmol) were placed together in a J-young NMR tube and dissolved in C_6D_6 (500 μL). The resulting mixture was analyzed by ^{31}P NMR spectroscopy with a capillary sealing H_3PO_4 (85 wt % in H_2O , diluted with 100-fold D_2O) as an internal standard (0.70 ppm). In the case of **2**, a set of signals probably derived from a structural isomer (~10%) was also observed in the ^{31}P spectrum of $2\cdot(\text{O})\text{PEt}_3$.

3.10. X-Ray Diffraction Study and X-Ray Crystallographic Analysis

The crystals of **6** and **8** were mounted on the CryoLoop (Hampton Research Corp., California, USA) with a layer of light mineral oil and placed in a nitrogen stream at 143(1) K. The X-ray structural determinations of **6** were performed on a Rigaku/Saturn70 CCD diffractometers using graphite-monochromated Mo $\text{K}\alpha$ radiation ($\lambda = 0.71070 \text{ \AA}$) at 153 K, and processed using CrystalClear (Rigaku, Tokyo, Japan) [46,47]. The X-ray structural determinations of **8** were performed on a Rigaku/Saturn724+ CCD diffractometers using graphite-monochromated Mo $\text{K}\alpha$ radiation ($\lambda = 0.71075 \text{ \AA}$) at 153 K, and processed using CrystalClear (Rigaku) [46,47]. The structures were solved by a direct method and refined by full-matrix least-square refinement on F^2 . The structures of **6** and **8** were solved by direct methods (SHELXS-97 and SHELX 2018) [48]. Non-hydrogen atoms were anisotropically refined except for solvent atoms due to their disorder. Hydrogen atoms were included in the refinement on calculated positions riding on their carrier atoms. CCDC 1946453 (for **6**) and 1963268 (for **8**) contain the supplementary crystallographic data. These data can be obtained from The Cambridge Crystallographic Data Centre.

4. Conclusions

In conclusion, a new Al tethered diphosphine ligand **2** derived from 2-diphenylphosphino-6-isopropylphenol has been developed. The utility of **2** as a supporting ligand was demonstrated through complexation of **2** with $[\text{RhCl}(\text{nbd})]_2$ to give zwitterionic complex **6**. Moreover, reduction of **6** with KC_8 afforded heterobimetallic complexes **7** and **8** bearing an X-type PAIP pincer ligand. Further applications of **2** as a supporting ligand for transition-metal catalysis are under investigation.

Supplementary Materials: The following are available online at <http://www.mdpi.com/2304-6740/7/12/140/s1>. CIF Files and CheckCIF Files, The detailed experimental procedures and NMR spectra of each compounds. CCDC 1946453 (for **6**) and 1963268 (for **8**) contain the supplementary crystallographic data for this paper. These data can be obtained free of via <http://www.ccdc.cam.ac.uk/conts/retrieving.html>.

Author Contributions: K.S. and I.F. planned, conducted and analysed experiments. K.S. and Y.N. cowrote the manuscript. Y.N. directed the project.

Funding: This research was supported by the CREST program “Establishment of Molecular Technology towards the Creation of New Functions” (JPMJCR14L3) from the JST.

Acknowledgments: We thank Naofumi Hara for X-ray crystallographic analysis.

Conflicts of Interest: The authors declare no conflict of interest.

References

1. Fontaine, F.G.; Boudreau, J.; Thibault, M.H. Coordination Chemistry of Neutral (L_n)–Z Amphoteric and Ambiphilic Ligands. *Eur. J. Inorg. Chem.* **2008**, *2008*, 5439–5454. [[CrossRef](#)]

2. Amgoune, A.; Bourissou, D. σ -Acceptor, Z-type Ligands for Transition Metals. *Chem. Commun.* **2011**, *47*, 859–871. [[CrossRef](#)] [[PubMed](#)]
3. Bouhadir, G.; Bourissou, D. Complexes of Ambiphilic Ligands: Reactivity and Catalytic Applications. *Chem. Soc. Rev.* **2016**, *45*, 1065–1079. [[CrossRef](#)]
4. Yamashita, M. The Organometallic Chemistry of Boron-Containing Pincer Ligands based on Diazaboroles and Carboranes. *Bull. Chem. Soc. Jpn.* **2016**, *89*, 269–281. [[CrossRef](#)]
5. Sircoglou, M.; Bouhadir, G.; Saffon, N.; Miqueu, K.; Bourissou, D. A Zwitterionic Gold(I) Complex from an Ambiphilic Diphosphino-Alane Ligand. *Organometallics* **2008**, *27*, 1675–1678. [[CrossRef](#)]
6. Sircoglou, M.; Mercy, M.; Saffon, N.; Coppel, Y.; Bouhadir, G.; Maron, L.; Bourissou, D. Gold(I) Complexes of Phosphanyl Gallanes: From Interconverting to Separable Coordination Isomers. *Angew. Chem. Int. Ed.* **2009**, *48*, 3454–3457. [[CrossRef](#)]
7. Segawa, Y.; Yamashita, M.; Nozaki, K. Syntheses of PBP Pincer Iridium Complexes: A Supporting Boryl Ligand. *J. Am. Chem. Soc.* **2009**, *131*, 9201–9203. [[CrossRef](#)]
8. Spokoiny, A.M.; Reuter, M.G.; Stern, C.L.; Ratner, M.A.; Seideman, T.; Mirkin, C.A. Carborane-Based Pincers: Synthesis and Structure of SeBSe and SBS Pd(II) Complexes. *J. Am. Chem. Soc.* **2009**, *131*, 9482–9483. [[CrossRef](#)]
9. Harman, W.H.; Peters, J.C. Reversible H₂ Addition across a Nickel–Borane Unit as a Promising Strategy for Catalysis. *J. Am. Chem. Soc.* **2012**, *134*, 5080–5082. [[CrossRef](#)] [[PubMed](#)]
10. Hasegawa, M.; Segawa, Y.; Yamashita, M.; Nozaki, K. Isolation of a PBP-Pincer Rhodium Complex Stabilized by an Intermolecular C–H σ Coordination as the Fourth Ligand. *Angew. Chem. Int. Ed.* **2012**, *51*, 6956–6960. [[CrossRef](#)] [[PubMed](#)]
11. Masuda, Y.; Hasegawa, M.; Yamashita, M.; Nozaki, K.; Ishida, N.; Murakami, M. Oxidative Addition of a Strained C–C Bond onto Electron-Rich Rhodium(I) at Room Temperature. *J. Am. Chem. Soc.* **2013**, *135*, 7142–7145. [[CrossRef](#)] [[PubMed](#)]
12. Sircoglou, M.; Saffon, N.; Miqueu, K.; Bouhadir, G.; Bourissou, D. Activation of M–Cl Bonds with Phosphine–Alanes: Preparation and Characterization of Zwitterionic Gold and Copper Complexes. *Organometallics* **2013**, *32*, 6780–6784. [[CrossRef](#)]
13. Lin, T.P.; Peters, J.C. Boryl–Metal Bonds Facilitate Cobalt/Nickel-Catalyzed Olefin Hydrogenation. *J. Am. Chem. Soc.* **2014**, *136*, 13672–13683. [[CrossRef](#)] [[PubMed](#)]
14. Harman, W.H.; Lin, T.P.; Peters, J.C. A d¹⁰ Ni–(H₂) Adduct as an Intermediate in H–H Oxidative Addition across a Ni–B Bond. *Angew. Chem. Int. Ed.* **2014**, *53*, 1081–1086. [[CrossRef](#)]
15. Cowie, B.E.; Tsao, F.A.; Emslie, D.J.H. Synthesis and Platinum Complexes of an Alane-Appended 1,1'-Bis(phosphino)ferrocene Ligand. *Angew. Chem. Int. Ed.* **2015**, *54*, 2165–2169. [[CrossRef](#)]
16. Shih, W.C.; Gu, W.; MacInnis, M.C.; Timpa, S.D.; Bhuvanesh, N.; Zhou, J.; Ozerov, O.V. Facile Insertion of Rh and Ir into a Boron–Phenyl Bond, Leading to Boryl/Bis(phosphine) PBP Pincer Complexes. *J. Am. Chem. Soc.* **2016**, *138*, 2086–2089. [[CrossRef](#)]
17. Shih, W.C.; Ozerov, O.V. Selective *ortho* C–H Activation of Pyridines Directed by Lewis Acidic Boron of PBP Pincer Iridium Complexes. *J. Am. Chem. Soc.* **2017**, *139*, 17297–17300. [[CrossRef](#)]
18. Takaya, J.; Iwasawa, N. Synthesis, Structure, and Catalysis of Palladium Complexes Bearing a Group 13 Metalloligand: Remarkable Effect of an Aluminum-Metalloligand in Hydrosilylation of CO₂. *J. Am. Chem. Soc.* **2017**, *139*, 6074–6077. [[CrossRef](#)]
19. Saito, T.; Hara, N.; Nakao, Y. Palladium Complexes Bearing Z-type PAIP Pincer Ligands. *Chem. Lett.* **2017**, *46*, 1247–1249. [[CrossRef](#)]
20. Hara, N.; Saito, T.; Semba, K.; Kuriakose, N.; Zheng, H.; Sakaki, S.; Nakao, Y. Rhodium Complexes Bearing PAIP Pincer Ligands. *J. Am. Chem. Soc.* **2018**, *140*, 7070–7073. [[CrossRef](#)]
21. Saito, N.; Takaya, J.; Iwasawa, N. Stabilized Gallylene in a Pincer-Type Ligand: Synthesis, Structure, and Reactivity of PGa^IP–Ir Complexes. *Angew. Chem. Int. Ed.* **2019**, *58*, 9998–10002. [[CrossRef](#)] [[PubMed](#)]
22. Burlitch, J.M.; Leonowicz, M.E.; Petersen, R.B.; Hughes, R.E. Coordination of Metal Carbonyl Anions to Triphenylaluminum, -gallium, and -indium and the Crystal Structure of Tetraethylammonium Triphenyl(η^5 -cyclopentadienyl)dicarbonyliron)aluminate (Fe–Al). *Inorg. Chem.* **1979**, *18*, 1097–1105. [[CrossRef](#)]

23. Golden, J.T.; Peterson, T.H.; Holland, P.L.; Bergman, R.G.; Andersen, R.A. Adduct Formation and Single and Double Deprotonation of Cp*(PMe₃)Ir(H)₂ with Main Group Metal Alkyls and Aryls: Synthesis and Structure of Three Novel Ir–Al and Ir–Mg Heterobimetallics. *J. Am. Chem. Soc.* **1998**, *120*, 223–224. [[CrossRef](#)]
24. Braunschweig, H.; Gruss, K.; Radacki, K. Interaction between d- and p-Block Metals: Synthesis and Structure of Platinum–Alane Adducts. *Angew. Chem. Int. Ed.* **2007**, *46*, 7782–7784. [[CrossRef](#)]
25. Bauer, J.; Braunschweig, H.; Brenner, P.; Kraft, K.; Radacki, K.; Schwab, K. Late-Transition-Metal Complexes as Tunable Lewis Bases. *Chem. Eur. J.* **2010**, *16*, 11985–11992. [[CrossRef](#)]
26. Derrah, E.J.; Sircoglou, M.; Mercy, M.; Ladeira, S.; Bouhadir, G.; Miqueu, K.; Maron, L.; Bourissou, D. Original Transition Metal→Indium Interactions upon Coordination of a Triphosphine-Indane. *Organometallics* **2011**, *30*, 657–660. [[CrossRef](#)]
27. Rudd, P.A.; Liu, S.; Gagliardi, L.; Young V.G., Jr.; Lu, C.C. Metal–Alane Adducts with Zero-Valent Nickel, Cobalt, and Iron. *J. Am. Chem. Soc.* **2011**, *133*, 20724–20727. [[CrossRef](#)]
28. Devillard, M.; Nicolas, E.; Appelt, C.; Backs, J.; Mallet-Ladeira, S.; Bouhadir, G.; Slootweg, J.C.; Uhl, W.; Bourissou, D. Novel Zwitterionic Complexes Arising from the Coordination of an Ambiphilic Phosphorus–Aluminum Ligand to Gold. *Chem. Commun.* **2014**, *50*, 14805–14808. [[CrossRef](#)]
29. Devillard, M.; Nicolas, E.; Ehlers, A.W.; Backs, J.; Mallet-Ladeira, S.; Bouhadir, G.; Slootweg, J.C.; Uhl, W.; Bourissou, D. Dative Au–Al Interactions: Crystallographic Characterization and Computational Analysis. *Chem. Eur. J.* **2015**, *21*, 74–79. [[CrossRef](#)]
30. Wang, G.; Xu, L.; Li, P. Double N,B-Type Bidentate Boryl Ligands Enabling a Highly Active Iridium Catalyst for C–H Borylation. *J. Am. Chem. Soc.* **2015**, *137*, 8058–8061. [[CrossRef](#)]
31. Devillard, M.; Declercq, R.; Nicolas, E.; Ehlers, A.W.; Backs, J.; Saffon-Merceron, N.; Bouhadir, G.; Slootweg, J.C.; Uhl, W.; Bourissou, D. A Significant but Constrained Geometry Pt–Al Interaction: Fixation of CO₂ and CS₂, Activation of H₂ and PhCONH₂. *J. Am. Chem. Soc.* **2016**, *138*, 4917–4926. [[CrossRef](#)] [[PubMed](#)]
32. Cammarota, R.C.; Vollmer, M.V.; Xie, J.; Ye, J.; Linehan, J.C.; Burgess, S.A.; Appel, A.M.; Gagliardi, L.; Lu, C.C. A Bimetallic Nickel–Gallium Complex Catalyzes CO₂ Hydrogenation via the Intermediacy of an Anionic d¹⁰ Nickel Hydride. *J. Am. Chem. Soc.* **2017**, *139*, 14244–14250. [[CrossRef](#)] [[PubMed](#)]
33. Wang, G.; Liu, L.; Wang, H.; Ding, Y.S.; Zhou, J.; Mao, S.; Li, P. N,B-Bidentate Boryl Ligand-Supported Iridium Catalyst for Efficient Functional-Group-Directed C–H Borylation. *J. Am. Chem. Soc.* **2017**, *139*, 91–94. [[CrossRef](#)] [[PubMed](#)]
34. Shi, Y.; Gao, Q.; Xu, S. Chiral Bidentate Boryl Ligand Enabled Iridium-Catalyzed Enantioselective C(sp³)–H Borylation of Cyclopropanes. *J. Am. Chem. Soc.* **2019**, *141*, 10599–10604. [[CrossRef](#)]
35. Hicks, J.; Mansikkamäki, A.; Vasko, P.; Goicoechea, J.M.; Aldridge, S. A Nucleophilic Gold Complex. *Nat. Chem.* **2019**, *11*, 237–241.
36. Allred, A.L.; Rochow, E.G. A Scale of Electronegativity Based on Electrostatic Force. *J. Inorg. Nucl. Chem.* **1958**, *5*, 264–268. [[CrossRef](#)]
37. Beckett, M.A.; Strickland, G.C.; Holland, J.R.; Varma, K.S. A Convenient n.m.r. Method for the Measurement of Lewis Acidity at Boron Centres: Correlation of Reaction Rates of Lewis Acid Initiated Epoxide Polymerizations with Lewis Acidity. *Polymer* **1996**, *37*, 4629–4631. [[CrossRef](#)]
38. Beckett, M.A.; Brassington, D.S.; Coles, S.J.; Hursthouse, M.B. Lewis Acidity of Tris(pentafluorophenyl)borane: Crystal and Molecular Structure of B(C₆F₅)₃·OPEt₃. *Inorg. Chem. Commun.* **2000**, *3*, 530–533. [[CrossRef](#)]
39. Maruoka, K.; Itoh, T.; Yamamoto, H. Methylaluminum Bis(2,6-di-*tert*-butyl-4-alkylphenoxide). A New Reagent for Obtaining Unusual Equatorial and Anti-Cram Selectivity in Carbonyl Alkylation. *J. Am. Chem. Soc.* **1985**, *107*, 4573–4576. [[CrossRef](#)]
40. Maruoka, K.; Itoh, T.; Sakurai, M.; Nonoshita, K.; Yamamoto, H. Amphiphilic Reactions by Means of Exceptionally Bulky Organoaluminum Reagents. Rational Approach for Obtaining Unusual Equatorial, Anti-Cram, and 1,4 Selectivity in Carbonyl Alkylation. *J. Am. Chem. Soc.* **1988**, *110*, 3588–3597. [[CrossRef](#)]
41. Batsanov, S.S. Van der Waals Radii of Elements. *Inorg. Mater.* **2001**, *37*, 871–885. [[CrossRef](#)]
42. Wassenaar, J.; Siegler, M.A.; Spek, A.L.; Bruin, B.; Reek, J.N.H.; Vlugt, J.I. Versatile New C₃-Symmetric Tripodal Tetraphosphine Ligands; Structural Flexibility to Stabilize Cu^I and Rh^I Species and Tune Their Reactivity. *Inorg. Chem.* **2010**, *49*, 6495–6508. [[CrossRef](#)] [[PubMed](#)]
43. Abel, E.W.; Bennett, M.A.; Wilkinson, G. Norbornadiene–Metal Complexes and Some Related Compounds. *J. Chem. Soc.* **1959**, 3178–3182. [[CrossRef](#)]

44. Pangborn, A.B.; Giardello, M.A.; Grubbs, R.H.; Rosen, R.K.; Timmers, F.J. Safe and Convenient Procedure for Solvent Purification. *Organometallics* **1996**, *15*, 1518–1520. [[CrossRef](#)]
45. Ihori, Y.; Yamashita, Y.; Ishitani, H.; Kobayashi, S. Chiral Zirconium Catalysts Using Multidentate BINOL Derivatives for Catalytic Enantioselective Mannich-Type Reactions; Ligand Optimization and Approaches to Elucidation of the Catalyst Structure. *J. Am. Chem. Soc.* **2005**, *127*, 15528–15535. [[CrossRef](#)]
46. Pflugrath, J.W. Rigaku Corporation, 1999, and CrystalClear Software User's Guide, Molecular Structure Corporation, 2000. *Acta Crystallogr. D* **1999**, *55*, 1718–1725. [[CrossRef](#)]
47. Pflugrath, J.W. The Finer Things in X-ray Diffraction Data Collection. *Acta Crystallogr.* **1999**, *55*, 1718–1725. [[CrossRef](#)]
48. Sheldrick, G.M. A Short History of SHELX. *Acta Crystallogr.* **2008**, *64*, 112–122. [[CrossRef](#)]



© 2019 by the authors. Licensee MDPI, Basel, Switzerland. This article is an open access article distributed under the terms and conditions of the Creative Commons Attribution (CC BY) license (<http://creativecommons.org/licenses/by/4.0/>).